Wide-Angle Alternating-Direction Implicit Finite-Difference Beam Propagation Method

Ella V. Bekker, *Member, IEEE*, Phillip Sewell, *Senior Member, IEEE*, Trevor M. Benson, *Senior Member, IEEE*, and Ana Vukovic, *Member, IEEE*

***Abstract*—An alternating direction implicit (ADI), scheme for the wide-angle finite-difference beam propagation method (FD-BPM) based on the wide angled Pade multistep method is presented. The scheme incorporates an iterative technique for correction of the operator splitting error. The resulting equations are efficiently solved by the Thomas algorithm for tri-diagonal band matrices. The dispersion characteristics, accuracy and stability of the scheme is verified analytically and numerically for the cases of a plane wave propagating at fixed angle to the assumed propagation direction of the algorithm and the three dimensional angled propagation of a Gaussian beam. The computational requirements of the method are assessed against a standard wide-angle Pade multistep method that uses direct and iterative sparse matrix solvers.**

***Index Terms*—Finite-difference methods, integrated optics, Pade approximants, wide-angle beam propagation.**

I. Introduction

THE finite-difference beam propagation method (FD-BPM) is a well established technique for modeling optical and photonics devices in both frequency and time domains [1]. The complexity of modern optical and photonics devices has substantially increased over the last decade, with high index contrast waveguides desirable for high density integration of optical devices and circuits. Many modern photonic devices and components such as arrayed waveguide gratings (AWGs) require the modeling of vectorial fields, wide angled propagation, reflections and/or bi-directional propagation in three spatial dimensions. This substantially increases both the complexity and the computational requirements of the FD-BPM [2].

A well-established approach for modeling wide-angle propagation in the FD-BPM is by introducing Pade approximants for the transverse operator and a multistep evaluation method [3]. However, in the case of three-dimensional (3D) simulations this method results in huge sparse matrices that are solved by either direct matrix solvers or faster iterative indirect solvers like the bi-conjugate gradient stabilized method [4]. Indirect solvers require an appropriate sparse matrix preconditioner, and convergence is not guaranteed in the case of wide-angled structures.

Presently, two different approaches are used to reduce the computational requirements of the 3D FD-BPM. The three-level schemes like Du-Fort Frankel (DFF), [5], enable larger step sizes but have conditional stability. Alternatively, a fast implicit solver like the alternating direction implicit (ADI) scheme results in a splitting of the differential operator into two directional components, substantially reducing the matrix problem size and increasing the computational speed of the method. The major drawback of the scheme is that the actual splitting of the operator introduces a zeroth order splitting error term that can be of the order of the Pade approximation itself. Reduction of the splitting error term to the $O(\Delta z)$ order, where Δz is the longitudinal step size, has been done by implementing Pade approximants and their ADI splitting for only one of the transverse (horizontal) directions [6]. A 3D horizontally wide-angle FD-BPM was formulated in [7] which used an ADI scheme and a multistep method for higher order Pade approximants and made use of the Douglas scheme in order to increase the order of derivatives approximation to 4. Representation of the Pade approximants by partial fractions is used in [8], and makes the scheme amenable to parallel computing techniques. In this approach an iterative method is proposed in which an adequate pre-conditioner based on a Pade (1,1) expansion is used to decrease the number of iterations [8]. An alternative approach to model wide angled propagation using ADI splitting, reported in [9]–[11], also increases the computational speed of the ADI method but limits the wide angled nature to a Pade (1,1) approximation.

In this paper a new iterative ADI scheme for wide-angle wave propagation based on Pade approximants and a multistep method is proposed. This approach results in tridiagonal matrices that can be easily solved using the Thomas algorithm. An iterative technique is used to correct for the operator splitting error by introducing adequate polynomials. The paper is organized as follows: Section II outlines the theory behind the standard wide angled BPM method based on the Pade multistep method [3] and then proceeds with the implementation of the multistep method within the ADI method and the correction of the splitting error. Section III derives the dispersion characteristic of the proposed ADI method for the case of a plane wave. Section IV-A presents results for plane wave dispersion, and analyses the accuracy and stability requirements of the wide-angled ADI multistep method by comparing results with analytical ones and with those obtained using a standard wide-angled FD-BPM, [3]. Section IV-B presents results for

Manuscript received April 15, 2008; revised September 26, 2008. First published April 24, 2009; current version published July 01, 2009. This work was supported by the U.K. EPSRC under Grant EP/D068444/1.

E. V. Bekker is with Photon Design Ltd., Oxford OX4 1TW, U.K. (e-mail: ebekker@photond.com).

P. Sewell, T. M. Benson, and A. Vukovic are with the George Green Institute for Electromagnetics Research, School of Electrical and Electronic, University of Nottingham, University Park, Nottingham NG7 2RD, U.K. (e-mail: phillip.sewell@nottingham.ac.uk; trevor.benson@nottingham.ac.uk; ana.vukovic@nottingham.ac.uk).

Digital Object Identifier 10.1109/JLT.2009.2013219

the case of the propagation of an angled Gaussian beam, and compares them against analytical ones presented in [10], [11]. Finally, the computational requirements of the proposed methodology are compared against those for a wide-angled multistep FD-BPM method [3] that uses either direct or iterative sparse matrix solvers.

II. Theory

In this section the conventional multistep method using Pade approximants is reviewed, followed by the ADI formulation based on the multistep method and the correction of the splitting error. The methodology is developed for the 3D semi-vectorial TE polarization.

The 3D semi-vectorial wave equation is [12]

$$\frac{\partial^2 E}{\partial z^2} + L_t E = 0 \tag{1}$$

where E denotes the E_x (horizontal) electric field component, z is the propagation direction, L_t is a transverse operator of the form

$$L_t = \frac{\partial}{\partial x}\frac{1}{\varepsilon}\frac{\partial}{\partial x}\varepsilon + \frac{\partial^2}{\partial y^2} + k_0^2\mu\varepsilon \tag{2}$$

and ε and k_0 are the dielectric constant and the free space wavenumber, respectively.

After factorization of (1)

$$\left(\frac{\partial}{\partial z} + j\sqrt{\hat{L}_t}\right)\left(\frac{\partial}{\partial z} - j\sqrt{\hat{L}_t}\right)E = 0$$

the forward propagating waves are chosen

$$\left(\frac{\partial}{\partial z} + j\sqrt{\hat{L}_t}\right)E = 0.$$

Rewriting the last equation for the slowly-varying field amplitude of the field E, namely $\mathrm{E^s}$, we obtain

$$\left(\frac{\partial}{\partial z} - j\beta_0 + j\sqrt{\hat{L}_t}\right)E^s = 0, \quad E = E^s\exp(-j\beta_0 z)$$

where β_0 is the reference propagation constant. The reference propagation constant can be either chosen as a propagation constant along the axis (as the uniform media one or the effective index of the fundamental mode) or can be calculated in each propagation step as a Rayleigh quotient [13], shown in the equation at the bottom of the page. Introducing this new notation, the following equation can be derived:

$$\left(\frac{\partial}{\partial z} - j\beta_0(1 - \sqrt{1+\hat{T}})\right)E^s = 0 \qquad \text{with } \hat{T} = \frac{\hat{L}_t - \beta_0^2}{\beta_0^2}$$

from which one can see the operator T corresponds to the operator P/β_0^2 in [12].

Further, Pade approximants are used to represent the resulting square root of the transverse operator. The expressions obtained are identical to those presented in [12] for the corresponding operator P. After using the Crank-Nicolson scheme to obtain an equivalent finite-difference equation, the field at the next computational step is presented by a ratio of polynomials of the transverse operator T

$$E_{i+1}^s = \frac{\sum_{n=0}^{N}\xi_n T^n}{\sum_{n=0}^{N}\xi_n^* T^n}E_i^s \tag{3}$$

where the coefficients ξ and $\xi*$ are uniquely determined for any choice of the order N. The polynomials of $\hat{T}$ in (3) can be factorized to be presented as

$$E_{i+1}^s = \frac{k(T/\chi_1+1)(T/\chi_2+1)\cdots(T/\chi_n+1)}{k^*(T/\chi_1^*+1)(T/\chi_2^*+1)\cdots(T/\chi_n^*+1)}E_i^s \tag{4}$$

where the relationship between ξ and (χ, k) coefficients can be found numerically or analytically from the standard polynomial factorization [14]; the asterisk at ξ and χ denotes complex conjugation.

Using higher order Pade approximants (such as 3,3) causes the appearance of poles in the rational polynomials, giving the potential for instability. In order to avoid it a common technique of "rotating" the Pade approximants in the complex plane [15] was implemented as an option for higher orders of Pade schemes

$$\sqrt{1+\hat{T}} = e^{j\varphi/2}\sqrt{1+((1+\hat{T})e^{-j\varphi}-1)}$$

resulting in the corresponding wave equation

$$\left(\frac{\partial}{\partial z} - j\beta_0(1 - e^{j\varphi/2}\sqrt{1+\hat{T}_{\mathrm{higher}}})\right)E^s = 0$$
$$\hat{T}_{\mathrm{higher}} = (1+\hat{T})e^{-j\varphi} - 1.$$

Since the further derivations can still be implemented in a straightforward way, we do not make further reference to the polynomial rotation in the complex plane in the theory below.

Further, the multistep approach similar to that presented in [3] is employed

$$E_{i+\frac{m}{n}}^s = \frac{(T/\chi_m+1)}{(T/\chi_m^*+1)}E_{i+\frac{m-1}{n}}^s \tag{5}$$

where m denotes the mth fractional sub-step. Equation (4) can be solved for each partial step using a direct matrix solver [16] or

$$\beta_0^2 = \frac{\int_{-\infty}^{\infty}\{k^2n^2(x,y)|E(x,y)|^2 - |\partial E(x,y)/\partial x|^2 - |\partial E(x,y)/\partial y|^2\}dxdy}{\int_{-\infty}^{\infty}|E(x,y)|^2dxdy}.$$

an iterative bi-conjugate gradient technique [4]. The (4), (5) represent the Hadley's wide-angle technique [3], referred to below as "standard WA FD-BPM." In the case of complex 3D structures (5) results in very large sparse matrices for which direct solution is computationally heavy and iterative methods are often ill-preconditioned.

In this paper, the alternating direction implicit algorithm and a conventional second order Crank-Nicolson scheme have been implemented to fulfill the calculation of the fields on partial steps described by (5) and splitting the operator T as

$$T = T_x + T_y \tag{6}$$

where the operators T_x and T_y are defined as

$$T_x = \frac{1}{\beta_0^2}\left(\frac{\partial}{\partial x}\frac{1}{\varepsilon}\frac{\partial}{\partial x}\varepsilon + \frac{k_0^2\mu\varepsilon}{2} - \frac{\beta_0^2}{2}\right)$$
$$T_y = \frac{1}{\beta_0^2}\left(\frac{\partial^2}{\partial y^2} + \frac{k_0^2\mu\varepsilon}{2} - \frac{\beta_0^2}{2}\right).$$

Substituting (6) into (5) results in an intermediate mth step as

$$E^s_{i+\frac{m}{n}} = \frac{(T_x/\chi_m + 1)(T_y/\chi_m + 1)}{(T_x/\chi^*_m + 1)(T_y/\chi^*_m + 1)} E^s_{i+\frac{m-1}{n}}. \tag{7}$$

The splitting of the operator introduces errors T_xT_y/χ_m^2 and T_xT_y/χ_m^{*2} in the numerator and denominator of (7), respectively. The coefficients χ determine the splitting error which is equivalent to $\mathrm{O}(\Delta z^2)$ for the paraxial case and further depends on the factorization for the higher order Pade approximants. Thus the actual error may diminish the accuracy of the Pade approximation itself. To decrease the error, correction terms based on the error terms T_xT_y/χ_m^2 and T_xT_y/χ_m^{*2} are introduced into the intermediate step as

$$E^s_{i+\frac{m}{n}} = \frac{(T_x/\chi_m + 1)(T_y/\chi_m + 1) - T_xT_y/\chi_m^2}{(T_x/\chi^*_m + 1)(T_y/\chi^*_m + 1) - T_xT_y/\chi_m^{*2}} E^s_{i+\frac{m-1}{n}}. \tag{8}$$

However, mixing of the operators T_x and T_y in the denominator prohibits the use of Thomas' algorithm. In order to overcome this problem, an iterative approach, using the known field as the first approximation is suggested below. By solving (8) iteratively the result can be calculated as

$$E^s_{i+\frac{m}{n}} = C_\nu E^s_{i+\frac{m-1}{n}} \tag{9}$$

where the coefficients $C_\nu, \nu = 0, 1 \ldots N_{\mathrm{iter}}$ are conveniently given as in (10), shown at the bottom of the page. The iterative finite-difference scheme presented by (9), (10) combines the split left hand part, allowing use of the Thomas algorithm, and an un-split right hand part, which suggests the use of different schemes recalled in [17], such as Safronov's scheme, or variations of the Douglas and Gunn's scheme.

In this work, the correction term is included in one of the ADI half steps, which immediately introduces a new splitting error (see (11) at the bottom of the page).

To further correct the error, we introduce the polynomial P at each intermediate step C_ν to cancel the error, shown in (12) at the bottom of the page, where the polynomial has the form

$$P = \left(\left(\frac{\chi_0}{\chi_1}\right)^2 - \left(\frac{\chi_0^*}{\chi_1^*}\right)^2 C_{\nu-1}\right) \times T_xT_y(V - V^2 + V^3 - V^4)$$

with

$$V = \left(\frac{\chi_0}{\chi_1}\right) T_x. \tag{13}$$

In order to ensure the order of error introduced by the polynomials is smaller than that of the iteration technique, the order of the polynomials chosen has to be higher than the number of the iterations itself. As one can see from (11) and (12), the iterations will be done only in one of the half steps of the ADI scheme. The polynomial calculations do not compromise the computational efficiency of the ADI method, as they only require six coefficients to be added when multiplying fields. Furthermore the

$$C_0 = \frac{(T_x/\chi_m + 1)(T_y/\chi_m + 1) - \left(\chi_m^{-2}T_xT_y - \chi_m^{*-2}T_xT_y\right)}{(T_x/\chi^*_m + 1)(T_y/\chi^*_m + 1)}$$
$$C_\nu = \frac{(T_x/\chi_m + 1)(T_y/\chi_m + 1) - \left(\chi_m^{-2} - \chi_m^{*-2}C_{\nu-1}\right)T_xT_y}{(T_x/\chi^*_m + 1)(T_y/\chi^*_m + 1)} \tag{10}$$

$$C_\nu = \frac{(T_x/\chi_m + 1)\left(T_y/\chi_m + 1 - \left(\chi_m^{-2} - \chi_m^{*-2}C_{\nu-1}\right)T_xT_y\right) + \mathrm{error}}{(T_x/\chi^*_m + 1)(T_y/\chi^*_m + 1)}. \tag{11}$$

$$C_\nu = \frac{(T_x/\chi_m + 1)\left(T_y/\chi_m + 1 - \left(\chi_m^{-2} - \chi_m^{*-2}C_{\nu-1}\right)T_xT_y + P\right)}{(T_x/\chi^*_m + 1)(T_y/\chi^*_m + 1)} \tag{12}$$

coefficients are recalculated only in those regions where there are refractive index changes.

The introduced ADI scheme described by equations (9,12) with $\nu = 0$ (this corresponds to no iteration of the ADI scheme) is referred further in the text as "ADI WA FD-BPM corrected" and the same ADI scheme with a few iterations $(\nu > 0)$ is referred as "ADI WA FD-BPM corrected and iterated."

In the vectorial case, the cross term derivatives of the transverse operator cannot be split. The finite difference representation of the terms has to be implemented using the previous propagation step field components with its following iterative update implemented as a part of the last term in (10). Consequently, an additional term will be introduced into the polynomial as well.

III. Dispersion Analysis

In this section the dispersion analysis of the new iterative ADI method based on the Pade multisteps is derived. The analytical form for the scheme dispersion is obtained when the field E is substituted by the monochromatic plane wave of the form

$$E = e^{j(\omega t - \Delta\beta l \Delta z - k_x n_r p \Delta x - k_y n_r q \Delta y)} \tag{14}$$

where $\Delta\beta = \beta - \beta_0, n_r$ is the refractive index, l, p and q are integers. If the plane wave is propagating at an angle α with respect to the z-axis and angle φ with respect to the x-axis, the projections of the k_0 vector on to the x, y and z axes are

$$\begin{aligned} k_x &= k_0 \sin\alpha\cos\varphi, \quad k_y = k_0 \sin\alpha \sin\varphi \\ k_z &= k_0 \cos\alpha. \end{aligned} \tag{15}$$

Substituting (14) into (4) and using

$$E_{i+1}^s = e^{j\Delta\beta\Delta z} E_i^s$$

the propagation constant β, can be found as

$$\beta = \beta_0 + \frac{1}{j\Delta z} \times \ln\left[\frac{(T/\chi_1 + 1)(T/\chi_2 + 1)\cdots(T/\chi_n + 1)}{(T/\chi_1^* + 1)(T/\chi_2^* + 1)\cdots(T/\chi_n^* + 1)}\right] \tag{16}$$

where β_0 is found here as $\beta_0 = k_z n$, and the transverse operator T is found as [19]

$$T = \frac{1}{\beta_0^2}\left(-\frac{4}{\Delta x^2}\sin^2\left(\frac{k_x\sqrt{\varepsilon}\Delta x}{2}\right) - \frac{4}{\Delta y^2}\sin^2\left(\frac{k_y\sqrt{\varepsilon}\Delta y}{2}\right) + k_0^2\varepsilon - \beta_0^2\right). \tag{17}$$

The iterative ADI algorithm, suggested in this paper, results in the following dispersion relation:

$$\beta = \beta_0 + \frac{1}{j\Delta z}\ln\left[\prod_{m=1}^{N_{\text{Pade}}} C_{\nu,m}\right] \tag{18}$$

where $C_{\nu,m}$ describes the mth Pade approximation partial step of (12).

The dispersion analysis described here incorporates the finite difference representation of the derivative in propagation direction similarly to that presented in [19]. It would not be enough to analyze the dispersion characteristics of the transverse operator itself, as it was done in [3], as it would not allow us to assess the influence of the operator splitting, which is performed on the resulting finite difference operator. However, in our analysis we will occasionally use the representation of transverse operator corresponding to $(\Delta\mathrm{x} \to 0, \Delta\mathrm{y} \to 0)$ as in [3]: $T = \sin^2(\alpha)$ and it is noted that the operator P of [3] corresponds to $\mathrm{T} * \beta_0^2$.

IV. Results

In this section, the plane wave dispersion of the new wide angled ADI scheme is compared with analytical values obtained from the analysis presented in Section III and also with the dispersion of the standard wide-angle BPM method of [12]. The stability issues of the proposed method are also discussed. Secondly, the dispersion of a Gaussian beam propagating in a uniform medium is analyzed. Finally, the computational requirements of the new BPM method are compared to those of [3], [12] that use either direct [16] or indirect [4] sparse matrix solvers. In all simulations a perfectly matched layer is implemented to model open boundaries [18]. For clarity, the analysis is limited to the first three orders of the Pade approximants.

A. Dispersion of a Plane Wave

In this section the dispersion characteristic given by (16), (18) is presented. Using the formulae of Section III the stability of the proposed multistep wide-angled ADI FD-BPM iterative scheme is compared to that of the standard multistep wide-angled BPM of [12]. Angular plane wave propagation in an homogeneous medium is considered and the semi-vectorial method introduced reduces in this case to the scalar one used by Hadley [12], allowing direct comparison of phase error calculated by two methods.

Similarly to [12], Fig. 1 shows the phase error obtained with variety propagators relative to the exact value of $-2\mathrm{j}\beta_0\sin^2(\alpha/2)$, where α is the propagation angle. The solid lines of Fig. 1(a) correspond to the $(\Delta\mathrm{x} \to 0, \Delta\mathrm{y} \to 0)$ representation of the operator T resulting in the same expressions and graphs as presented in [12], but shown here on a logarithmic scale. It is observed that the angles when the phase error is under 3.e-3 correspond to 5, 27 and 65 degrees for Paraxial, Pade(1,1) ,and Pade(3,3) approximants, respectively. The phase error of 3.e-3 mentioned corresponds to that which can reasonably be distinguished from zero by eye on the linear graph presented in [12].

However, for finite values of $\Delta\mathrm{x}, \Delta\mathrm{y}$ the accuracy of approximation itself can be undermined causing the errors similar to those of lower order approximations for smaller angles, as one can see from the dotted and dashed lines of Fig. 1(a).

For this analysis, the plane wave is assumed to propagate in a uniform medium of refractive index $n_r = 1$ at an operating wavelength of 1.15 μm. Unless specified additionally, the transverse discretization employed is $\Delta x = \Delta y = 0.01\,\mu$m and

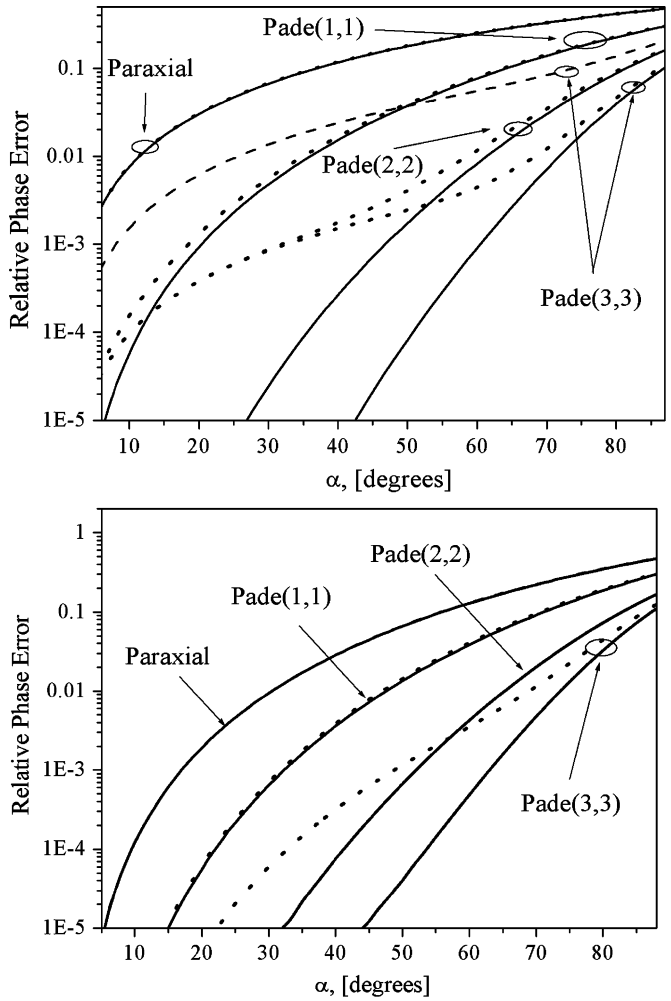

Fig. 1. Phase Error incurred by the use of the operators shown for propagation of a plane wave at various angles with respect to the z axis: solid line ($\Delta x \to 0, \Delta y \to 0$), dashed lines: $\Delta x = \Delta y = 0.2\,\mu$m, dotted lines: $\Delta x = \Delta y = 0.05\,\mu$m. (a) error incurred purely due to transverse operator expansion by Pade approximants, without the finite difference representation of the derivative in propagation direction (dispersion analysis similar to [12]); (b) error when using dispersion analysis described in Section III.

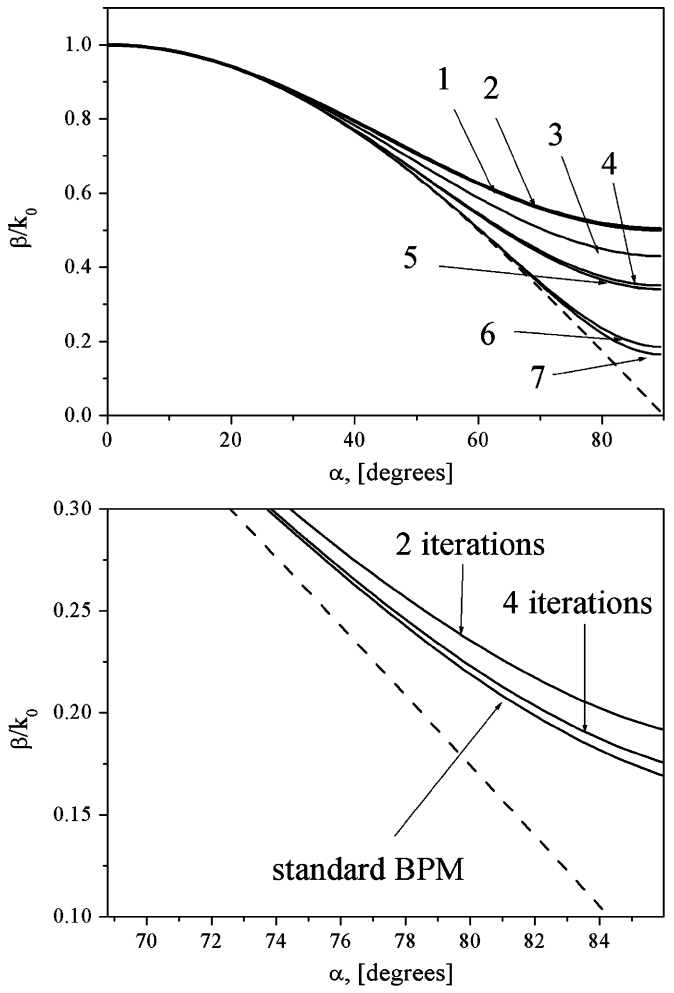

Fig. 2. Numerical dispersion characteristics: (a) (1)—paraxial FD-BPM, (2)—paraxial ADI FD-BPM, (3)—Pade(1,1) conventional ADI, (4)—Pade(1,1) ADI WA FD-BPM corrected (not iterated), (5)—Pade(1,1) standard WA FD-BPM, (6)—Pade(3,3) ADI WA FD-BPM corrected and iterated to converge; (7)—Pade(3,3) standard WA FD-BPM; (b) standard WA FD-BPM Pade(3,3) and ADI WA FD-BPM corrected and iterated Pade(3,3) with 2 and 4 iterations. Dashed lines here correspond to $\beta_0 = k_z n / k_0$.

the longitudinal step size is $\Delta z = 0.1\,\mu$m. The plane wave is assumed to propagate at an angle α with respect to the propagation axis.

Similar results, calculated for dispersion characteristics taking into account the finite difference representation of the propagation direction derivative (16)–(18) are presented in Fig. 1(b). As one can see the discretization of the derivative in the propagation direction which was not investigated in [12] can affect the accuracy of the different orders of approximations: the curves are shifted to higher angles compared to the dispersion characteristics of the Fig. 1(a), but the influence of the transverse operator discretization is similar, often undermining the accuracy of approximation itself. Furthermore, the same effect is observed when varying the value of the longitudinal step—the effect that may limit the size of the longitudinal step to be used in ordinary WA FDM to achieve higher accuracy, corresponding to the Pade approximation itself.

In the following results we will concentrate on analysis of propagation constant itself rather than the phase error. From (16), (18) the dependence of the propagation constant on the propagation angle α is shown in Fig. 2(a) and (b) for different Pade orders. Curves 1 and 2 denote the paraxial FD-BPM method and paraxial ADI FD-BPM (namely Pade(1,0)), results respectively. It can be seen that they are almost identical as the splitting error is proportional to the square of the longitudinal step, Δz. For the case of a Pade(1,1) approximation the result obtained using the standard FD-BPM method is given by curve 5, [12]. Curves 3 and 4 denote the Pade(1,1) ADI schemes without and with the splitting error correction respectively. It can be seen that when the correction is implemented the ADI scheme gives more accurate results than its uncorrected alternative, i.e., results of curve 4 are much closer to those of curve 5. This improvement is obtained without increasing the computational time or memory consumption over those of the conventional ADI scheme. Curves 6 and 7 show results for a multistep Pade (3,3) approximation, calculated using ADI corrected by a polynomial of third order implementing 2 iterations and the method of [12], respectively. Once again the

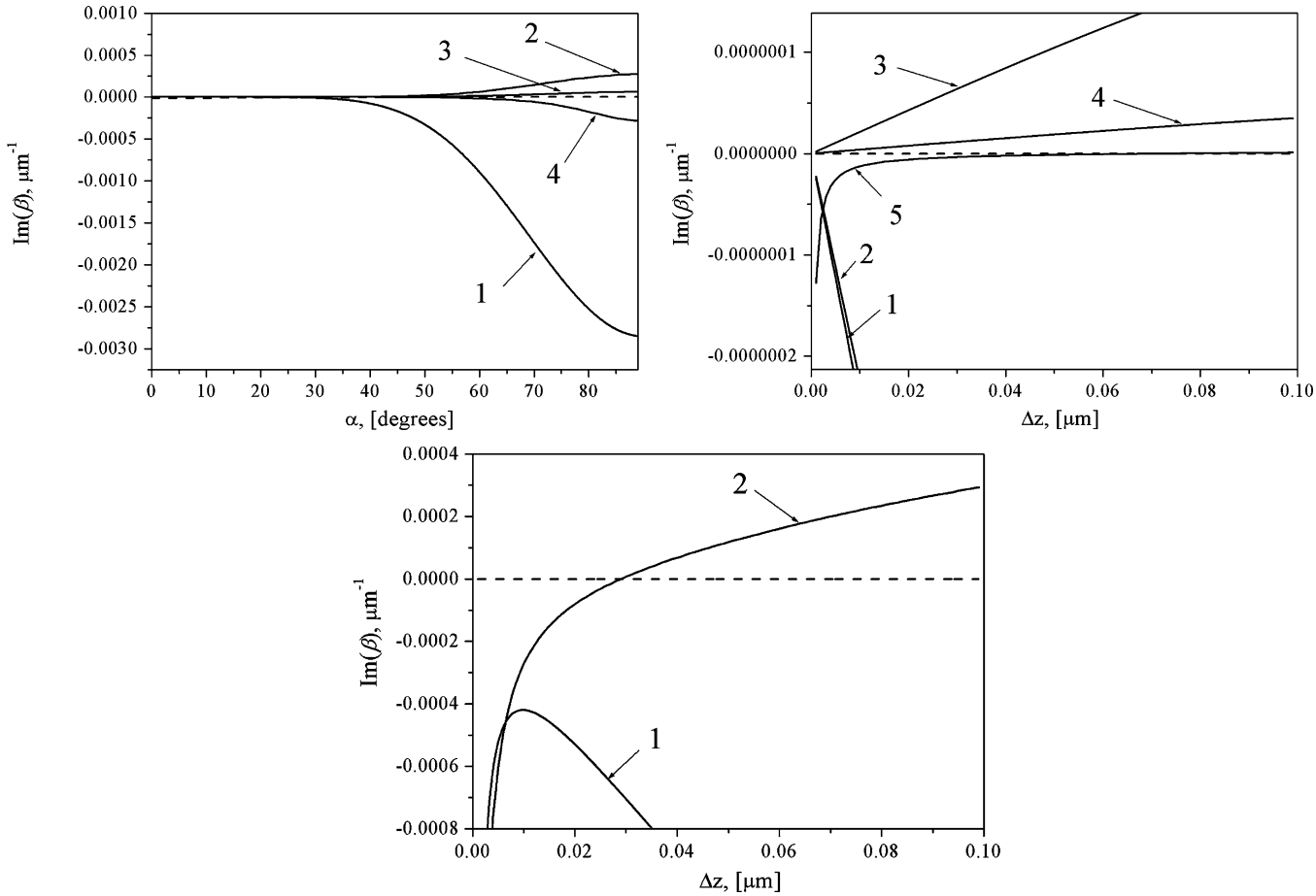

Fig. 3. Dissipative dispersion characteristics ($\lambda = 1.15\,\mu$m, $\Delta x(\Delta y) = 0.02\,\mu$m, dashed line corresponds to the standard WA FD-BPM): (a) (1)—Pade(1,1) using ADI WA FD-BPM corrected; (2)—Pade(1,1) using ADI WA FD-BPM corrected and iterated to convergence (5 and 8 iterations); (3)—Pade(2,2) using ADI WA FD-BPM corrected and iterated to convergence; (4)—Pade(3,3) using ADI WA FD-BPM corrected and iterated to convergence; $\Delta z = 0.02\,\mu$m. (b) (1)—Pade(1,1) using ADI WA FD-BPM corrected, (3)—and converged (5 and 8 iterations); (2)—Pade(2,2) using ADI WA FD-BPM corrected, (4)—and converged (5 and 8 iterations); (5)—Pade(3,3) using ADI WA FD-BPM corrected and iterated to converge (5 and 8 iterations); $\alpha = 30°$. (c) (1)—Pade(3,3) using ADI WA FD-BPM corrected and iterated (3 iterations); (2)—Pade(3,3) using ADI WA FD-BPM corrected and iterated to converge (5 and 8 iterations) $\alpha = 90°$.

results are in good agreement and, as expected, they approach the analytical results (dashed curve on the graph) for wider propagation angle as the Pade order is increased.

As one can see from the results for first order Pade approximant the corrected ADI WA FD-BPM is a sufficient approximation of the standard one, and no iterative correction is needed. The same is found to be true for the second order of Pade approximant as well. Fig. 2(b) compares dispersion results for the Pade(3,3) approximant in more detail. In this figure results obtained using the corrected multistep Pade(3,3) ADI with 2 and 4 iterations are compared to those obtained using the standard Pade(3,3) scheme of [12]. The comparison illustrates a general observation that for higher order Pade approximants (here, Pade (3,3)) the corrected multistep ADI scheme requires more iterations to reach the accuracy of the standard Crank-Nicolson FD-BPM scheme of [12].

The results of the numerical dispersion calculations presented in the Fig. 2 demonstrate the ability to use ADI-like schemes for higher order Pade approximants achieving similar accuracy in the wide-angle field representation as the standard WA FD-BPM. However, the exploitation of the ADI-like schemes greatly reduces the computational resource as will be discussed in detail in Section IV-C. The angular limitations of Pade approximants are not straightforwardly seen from the graph, however can be easily checked while calculating the phase error, as demonstrated in Fig. 1 and in our previous results [21].

Fig. 3 addresses stability issues involved in the multistep ADI schemes by analyzing the imaginary part of the propagation constant, which is responsible for the numerical loss or gain and thus may affect the stability of the scheme. Our results will be demonstrated on the example of Pade (1,1) and Pade(3,3) approximants. The Pade(1,1) results are presented for the ADI WA FD-BPM corrected but not iterated scheme. As already shown, this scheme does not need any iterations to improve the dispersion characteristics. The Pade(3,3) results are used to represent the common behavior of the higher order Pade approximation schemes. Fig. 3(a) and (b) compare the Pade(1,1), Pade(2,2) and Pade(3,3) schemes, whilst the Fig. 3(c) concentrates on the comparison of Pade(3,3) schemes with different number of iterations involved.

Fig. 3(a) shows how the imaginary part of β varies with the angle of propagation. While, as shown before [12], the standard WA FD-BPM does not introduce any numerical loss or

gain to the calculation (dashed line), the ADI WA FD-BPM corrected schemes may bring numerical loss which increases with the angle of propagation. For the particular case of Fig. 2(a) the numerical loss of the Pade(1,1) corrected scheme (curve 1) is higher than that for the Pade(3,3) one (curve 4).

The numerical loss would not cause any instability of the scheme (only additional dissipation) and in any case appears for the higher angles for which the current Pade approximations are not sufficient. For the ADI WA FD-BPM corrected and converged schemes of Pade(1,1) and Pade(2,2), the solution is unstable.

Fig. 3(b) shows the imaginary part of the propagation constant as a function of the longitudinal step size for a particular case of a plane wave propagating at $\alpha = 30$ degrees, mesh size $\Delta x = \Delta y = 0.02\,\mu$m and operating wavelength $\lambda = 1.15\,\mu$m. As one can see the numerical loss observed for the Pade(1,1) and Pade(2,2) schemes remarkably increases with the step size. This effect may in practice limit the step size that can be used with a Pade(1,1) scheme so as to minimize the numerical loss. For example, the losses for the Pade(1,1) scheme $\alpha = 30^\circ$ ($\Delta z = 0.02\,\mu$m) correspond to 0.004 dB/mm. Interestingly, the limiting factor for the longitudinal step in the Pade(3,3) scheme is not the growth of the numerical loss but rather the fact that for a particular value of Δz the imaginary value of the β curve becomes positive. This results in numerical gain, indicative of the scheme's instability. This limits the size of the longitudinal step Pade(3,3) that can be chosen. As one can see from the curve 3 and 4 of Fig. 3(b), converged schemes for Pade(1,1) and Pade(2,2) are unstable for any size of longitudinal step, and can not be used. However the corrected ADI WA FD-BPM scheme for Pade(1,1) gives good approximation as can be seen from results shown in Fig. 2(a).

Fig. 3(c) further investigates this behavior for the highest possible angle of 90° and compares converged and non-converged results for the Pade(3,3) ADI WA FD_BPM corrected and iterated methods. The simulation parameters are $\Delta x = \Delta y = 0.02\,\mu$m and operating wavelength $\lambda = 1.15\,\mu$m, as for Fig. 3(b). For higher angles of propagation the numerical loss or gain of the converged schemes (curve 2) is higher. However, appropriate choice of Δz can ensure stability. The non-converged Pade(3,3) scheme (curve 1) remains a dissipative scheme for any longitudinal step size.

For a converged and iterated ADI WA FD-BPM Pade(3,3) scheme, the loss for propagation at 60° will be about 0.005 dB/mm, and for propagation at 30° about 5×10^{-7} dB/mm when using a longitudinal step size of 0.02 μm. These errors are sufficiently small to have little impact on the physical interpretation of the phenomena described.

The curves in Fig. 3 also show that there is an optimal Δz for which the scheme has neither loss nor gain, implying that the introduced methodology has conditional stability. The conditions of the stability depend on the refractive index of the media, and in the case of waveguides it would depend on the effective refractive index found using say a Rayleigh quotient. This may suggest using an adaptive longitudinal step when simulating waveguides. Whilst we have not yet rigorously investigated the influence of refractive index contrast on stability and error, our preliminary investigations for a high index contrast angled rectangular waveguide [20] did not demonstrate any additional instabilities.

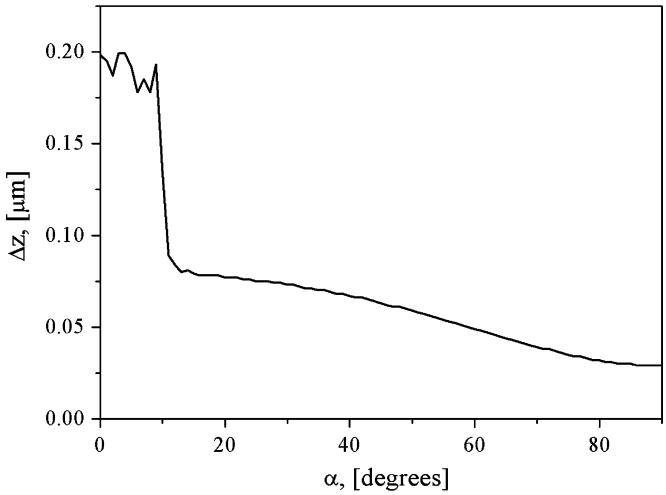

Fig. 4. Propagation step values corresponding to zero loss propagation described by converged ADI Pade(3,3) scheme.

Fig. 4 shows the value of the longitudinal step size obtained for zero numerical loss or gain for different angles of field propagation. It can be seen that the zero loss or gain criterion requires smaller longitudinal step size for higher angles of field propagation.

It can be concluded from Figs. 2, 3(c), and 4 that the new algorithm requires longitudinal step size of the order of 0.03 μm-0.1 μm. This is also an appropriate choice for many applications.

B. Numerical Simulations of Angled Gaussian Beam

In this section numerical results for the full 3D propagation of an angled Gaussian beam in an homogeneous medium obtained using the proposed multistep ADI method are compared with analytical results and those presented in [10], [11].

The initial Gaussian beam is located at the center of the coordinate system, (0, 0) of the computational window with x and y varying from -20 μm to 55 μm, and z varying from 0 μm to 60 μm. The transverse mesh size is $\Delta x = 0.15$ μm, $\Delta y = 0.15$ μm and the longitudinal step size is $\Delta z = 0.2$ μm. According to our estimations demonstrated on Fig. 3, the choice of the longitudinal step will result in a lossy scheme with numerical loss approximately $\sim 10^{-4}$ dB at $z = 60$ μm; this corresponds to a power loss of 10^{-5} which is deemed acceptable accuracy for this numerical experiment. The initial Gaussian beam width is 3 μm, and the angle of the beam propagation is 45° with respect to both the transverse x and y axes, and 30° with respect to the longitudinal z-axis. The operating wavelength is 0.85 μm. Fig. 5 shows the initial and the output field distribution of the Gaussian beam across the transverse x-y plane. The output field obtained using the ADI Pade(1,1) multistep method with error correction presented in this paper is compared with the analytical prediction. It can be seen that the analytical and multistep ADI results are in very good agreement. Furthermore, it can be observed that the coincidence of the output Gaussian beams calculated by the corrected Pade(1,1) scheme and the analytical solution is better than those shown for the Hoekstra scheme in

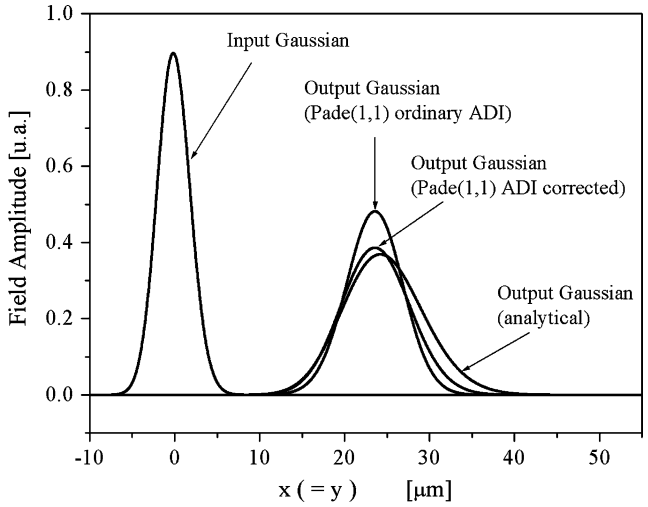

Fig. 5. Propagation of a Gaussian beam, showing the initial field, the analytic output field, and the output field calculated using a Pade(1,1) ADI WA FD-BPM corrected scheme. The results presented are along the diagonal x = y.

[10], [11]. Effectively, the proposed scheme requires the same number of ADI half steps as the Hoekstra scheme, but has an improved dispersion characteristic.

A comparison of Fig. 5 to the identical plot presented in [10] (calculated using the same parameters) shows that the present Pade(1,1) scheme gives results that are much closer to the analytical results. This is as expected since the dispersion curve of the Hoekstra scheme used in [10], curve 3 in Fig. 3(a), is poorer than that of curve 4 for the Pade(1,1) ADI WA FD-BPM corrected scheme.

To systematically assess the accuracy of the proposed methodology, the shift of the Gaussian peak, η_o, in the x-y plane and the standard deviation of the Gaussian beam, σ^2, are observed and compared with the analytical values which are found as

$$\eta_0 = \int_{-\infty}^{+\infty} \eta I(x,y)dxdy \tag{19}$$

and

$$\sigma^2_{\eta,\upsilon} = \int_{-\infty}^{+\infty} (\eta - \eta_0)^2 I(x,y)dxdy \tag{20}$$

where $I(x,y)$ is the intensity of the Gaussian beam and η is $x(y)$.

Fig. 6 shows the results for (a) the Gaussian peak and (b) the standard deviation of the Gaussian beam shift as a function of the angle α. For these results the mesh size used is $\Delta x = 0.425$ μm, $\Delta y = 0.425$ μm. The operating wavelength is 0.85 μm and z varies from 0 μm to 50 μm. For this, and subsequent examples a coarse transverse grid size is chosen. This is principally because in order to compare the efficacy of the new technique with that of a standard WA FD-BPM we will need to use a coarser mesh size to make the calculations by the standard method tractable. However, as already shown our higher order schemes can provide better wide-angle approximation than those presented in [9], [10] and for that reason the use of fine grid is less important. The initial Gaussian beam

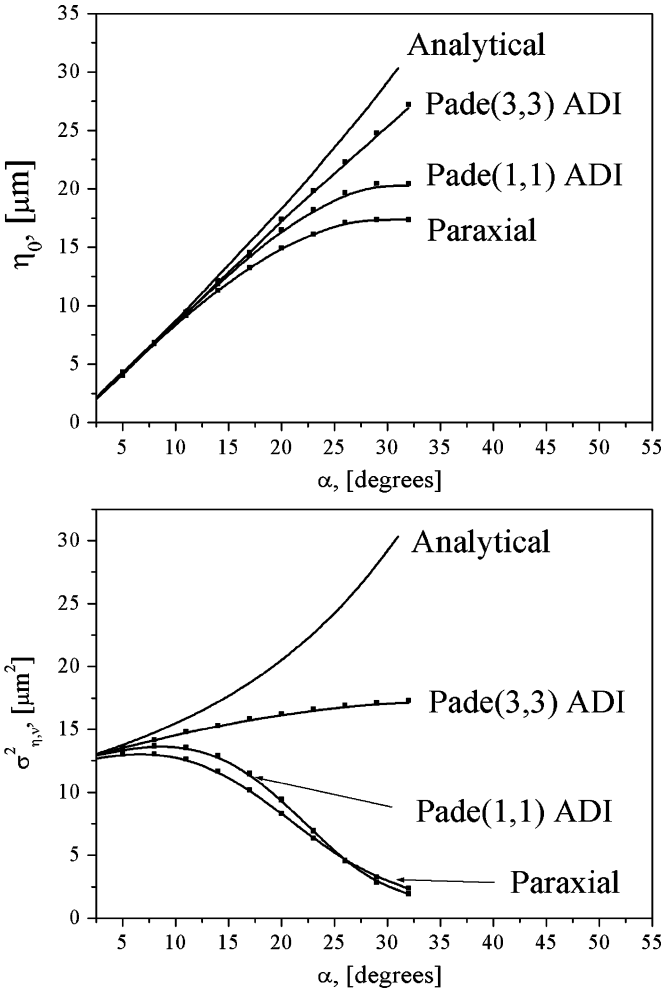

Fig. 6. (a) The shift of the peak of the Gaussian beam and (b) the standard deviation of the Gaussian beam. Results obtained with ADI WA FD-BPM corrected for paraxial case, Pade(1,1) and Pade(3,3) (solid lines) are compared against the analytical ones and ordinary multistep WA FDM (dot symbols).

width is 2 μm and the beam is angled with respect to the x and y axes at an angle of 45°. The results obtained using the proposed methodology are compared with the analytical values and the paraxial ADI scheme. The longitudinal step size is determined by the conditional stability of the higher order Pade ADI schemes (the longitudinal step must be under 0.029 μm for Pade(3,3) scheme) and the numerical loss of the Pade(1,1) scheme discussed in the descriptions of results in Figs. 3 and 5. Correspondingly, the longitudinal steps for the experiment were chosen to be $\Delta z = 2.5$ μm for paraxial ADI, $\Delta z = 0.25$ μm for Pade(1,1) and $\Delta z = 0.025$ μm for Pade(3,3). Fig. 6(a) shows that the higher order Pade approximants improve the accuracy of wide angled simulations and better predict the Gaussian peak shift. The results are similar to the ordinary multistep WA FD-BPM.

Fig. 6(b) shows that the standard deviation is a much more sensitive measure of the wide angular nature of the field and requires higher Pade order to achieve good agreement with analytical values. This is because the widening of the pulse is described by the field components propagating at higher angles to the axis than the beam itself, requiring higher Pade order.

TABLE I
MEMORY AND TIME RESOURCES, REQUIRED FOR SIMULATIONS OF HUNDRED STEPS PROPAGATION FOR PADE(1,1) APPROXIMATION (N DESCRIBES THE NUMBER OF TRANSVERSAL STEPS IN BOTH X AND Y DIRECTIONS)

	Iterative ADI		Bi-CSTAB		UMFPack	
N	RAM	Time	RAM	Time	RAM	Time
100	54Mb	16s.	crash	crash	90Mb	2m.30s.
150	60Mb	40s.	83Mb	1m.40s.	95Mb	6m.40s.
200	68Mb	1m.8s.	128Mb	3m.50s.	213Mb	17m.30s
300	88Mb	3m.10s.	400Mb	8m.20s.	408Mb	50 min.
400	154Mb	4m.20s.	440Mb	16m.40s.	755Mb	167min.
500	239Mb	7m.30s.	700Mb	30min.	1240Mb	300min.

C. Computational Requirements of the ADI Method Based on Pade Multisteps With Error Correction

This section assesses the computational memory and time requirements of 3D wide-angled multistep ADI technique based on Pade approximants against the standard wide-angled BPM multistep method using the direct method [14] (labeled as UMFPack) and the biconjugate gradient stabilized iterative technique [4] (labeled as Bi-CSTAB) for matrix solving. The simulation problem chosen is the Gaussian beam propagation given in Fig. 6.

Table I demonstrates the comparison of these techniques for Pade(1,1) approximation and for different values of the mesh size N where $N = N_x, N_y$ The iterative ADI and Bi-CSTAB techniques both demonstrate considerable improvement in the computation efficiency in comparison to the UMFPackage.

Furthermore, the iterative ADI technique requires less memory and is much faster when compared to the Bi-CSTAB technique.

V. CONCLUSION

A wide-angle ADI FD-BPM algorithm based on a Pade multistep method incorporating an iterative procedure to correct the operator splitting error is presented and assessed. The numerical dispersion characteristics of the proposed ADI scheme is derived and assessed for the case of plane wave propagation. It is shown that even without the iterative correction procedure the accuracy of the Pade (1,1) ADI with error correction is very close to that of original BPM based on multistep method [12]. The ADI based on higher order Pade approximants requires a few iterations for error correction to improve the accuracy. Unlike the standard WA FD-BPM, the stability of the algorithm is found to be conditional on the longitudinal step size. The conditional stability requires smaller longitudinal steps for higher angles of propagation. The choice of the longitudinal step size can also be made to satisfy the zero dispersion criteria. Furthermore, numerical simulations of the angled Gaussian beam propagation were performed and results compared against the analytical ones and those obtained under the paraxial approximation. As expected, the ADI WA FD-BPM corrected and iterated scheme improved the accuracy compared to the paraxial ADI scheme, converging to the results of standard WA FD-BPM. Finally, the computational requirements of the proposed methodology are compared against original Pade multistep method with either iterative BiConjugate Gradient or direct matrix solvers. The proposed iterative technique can significantly reduce computational requirements for the 3D simulations.

REFERENCES

[1] P. C. Lee, D. Schultz, and E. Voges, "Three-dimensional finite difference beam propagation algorithms for photonic devices," *J. Lightw. Technol.*, vol. 19, no. 12, pp. 1832–1838, 1992.

[2] P. Bienstman and R. Baets, "Optical modeling of photonic crystals and VCSELs using eigenmode expansion and perfectly matched layers," *Opt. Quan. Electron.*, vol. 33, no. 4–5, pp. 327–341, Apr. 2001.

[3] G. R. Hadley, "Multistep method for wide-angle beam propagation," *Opt. Lett.*, vol. 17, no. 24, pp. 1743–1745, Dec. 1992.

[4] S. H. Wei and Y. Y. Lu, "Application of Bi-CGSTAB to waveguide discontinuity problems," *IEEE Photon. Technol. Lett.*, vol. 14, no. 5, pp. 645–647, May 2002.

[5] P. Sewell, T. M. Benson, and A. Vukovic, "A stable DuFort Frankel beam-propagation method for lossy structures and those with perfectly matched layers," *J. Lightw. Technol.*, vol. 23, no. 1, pp. 374–381, Jan. 2005.

[6] J. Shibayama, T. Takahashi, J. Yamauchi, and H. Nakano, "A three-dimensional horizontally wide-angle noniterative beam propagation method based on the alternating-direction implicit scheme," *IEEE Photon. Technol. Lett.*, vol. 18, no. 5, pp. 661–663, Mar. 2006.

[7] J. Shibayama, T. Takahashi, J. Yamauchi, and H. Nakano, "A three-dimensional horizontally wide-angle beam propagation method based on the generalized Douglas scheme," *IEEE Photon. Technol. Lett.*, vol. 18, no. 23, pp. 2535–2537, Mar. 2006.

[8] S. L. Chui and Y. Y. Lu, "Wide-angle full-vector beam propagation method based on an alternating direction implicit preconditioner," *J. Opt. Soc. Am. A*, vol. 21, no. 3, pp. 420–425, Mar. 2004.

[9] H. J. W. M. Hoekstra, G. J. M. Krijnen, and P. V. Lambeck, "On the accuracy of the finite difference method for applications in beam propagating techniques," *Opt. Commun.*, vol. 94, pp. 506–508, 1992.

[10] C. Ma and E. V. Keuren, "A simple three-dimensional wide-angle beam propagation method," *Opt. Express*, vol. 14, no. 11, pp. 4668–4674, May 2006.

[11] C. Ma and E. V. Keuren, "A three-dimensional wide-angle BPM for optical waveguide structures," *Opt. Express*, vol. 15, no. 2, pp. 402–407, Jan. 2007.

[12] G. R. Hadley, "Wide-angle beam propagation using Pade approximant operators," *Opt. Lett.*, vol. 17, no. 2, pp. 1426–1428, Oct. 1992.

[13] S. Jungling and J. C. Chen, "A study and optimization of eigenmode calculations using imaginary-distance beam propagation method," *IEEE J. Quantum Electron.*, vol. 30, no. 9, pp. 2098–2105, 1994.

[14] B. E. A. Saleh and M. C. Teich, *Fundamentals of Photonics*. New York: Wiley, 1991, ch. 3, pp. 80–107.

[15] D. Yevick, "The application of complex Pade approximants to vector field propagation," *IEEE Photon. Technol. Lett.*, vol. 12, pp. 1636–1638, 2000.

[16] T. A. Davis, *Direct Methods for Sparse Linear Systems*. Philadelphia, PA: SIAM, 2006.

[17] S. McKee and A. R. Mitchell, "Alternating direction methods for parabolic equations in two space dimensions with mixed derivatives," *Comput. J.*, vol. 13, no. 1, pp. 81–86, Feb. 1970.

[18] J. P. Berenger, "A perfectly matched layer for the absorption of electromagnetic waves," *J. Comp. Phys.*, vol. 114, pp. 185–200, 1994.

[19] J. J. Lim, T. M. Benson, E. C. Larkins, and P. Sewell, "Wideband finite-difference-time-domain beam propagation method," *Microw. Opt. Technol. Lett.*, vol. 34, no. 4, pp. 243–247, Aug. 2002.

[20] R. Barrett, M. Berry, A. F. Chan, J. Demmel, J. Donato, J. Dongarra, V. Eijkhout, R. Pozo, C. Romine, and H. Vorst, *Templates for the Solution of Linear Systems: Building Blocks for the Iterative Methods*. Philadelphia, PA: SIAM, 1994.

[21] E. V. Bekker, P. Sewell, T. M. Benson, and A. Vukovic, "Wide-angle alternating-direction implicit finite-difference BPM," in *Proc. 9th Int. Conf. Transparent Opt. Netw. (ICTON 2007)*, vol. 1, pp. 250–254.

Ella Bekker (M'99) was born in Engels, Russia, in 1971. She received M.Sc. degree in optics and Ph.D. degree in laser physics from Saratov State University, Saratov, Russia, in 1997, and 2001, respectively.

She worked as a Research Scientist for a high-technology company for one year (2001–2002) in Saratov, Russia, and then joined the University of Nottingham, Nottingham, U.K., where she worked as a Postdoctoral Research Fellow from 2002 to 2007. Since 2007, she works for Photon Design Company, Oxford, U.K., as a Senior Developer of numerical modeling software for electromagnetics. Her research interests are in numerical modeling of nonlinear phenomena in optical waveguides and lasers.

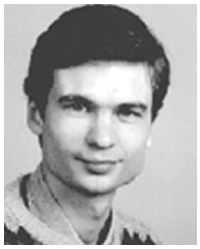

Phillip Sewell (M'89–SM'04) received the B.Sc. degree in electrical and electronic engineering (first-class honors) and Ph.D. degree from the University of Bath, Bath, U.K., in 1988 and 1991, respectively.

From 1991 to 1993, he was a Postdoctoral Fellow with the University of Ancona, Ancona, Italy. In 1993, he became a Lecturer with the School of Electrical and Electronic Engineering, University of Nottingham, Nottingham, U.K., where, in 2001, he became a Reader and, in 2005, a Professor of Electromagnetics.

Trevor M. Benson (M'95–SM'01) received the B.Sc. degree in physics (first-class honors) and the Ph.D. degree in electronic and electrical engineering from the University of Sheffield, Sheffield, U.K., in 1979 and 1982, respectively, and the D.Sc. degree from the University of Nottingham, Nottingham, U.K., in 2005.

After six years as a Lecturer at University College Cardiff, he joined the University of Nottingham, in 1989, and was promoted to Professor of Optoelectronics in 1996.

Dr. Benson is a Fellow of the Royal Academy of Engineering, the Institution of Engineering and Technology (IET), London, U.K., and the Institute of Physics. He has received the Electronics Letters and J. J. Thomson Premiums from the Institute of Electrical Engineers.

Ana Vukovic (M'97) was born in Nis, Yugoslavia, in 1968. She received the Diploma of Engineering in electronics and telecommunication from the University of Nis, Nis, Yugoslavia, in 1992 and the Ph.D. degree from the University of Nottingham, Nottingham, U.K., in 2000.

From 1999 to 2001, she was working as a Research Associate at the University of Nottingham where, in 2001, she joined the School of Electrical and Electronic Engineering as a Lecturer. Her research interests are in the area of electromagnetics, with particular emphasis upon applications in optoelectronics, microwaves and electromagnetic compatibility.